

The effects of palbociclib in combination with radiation in preclinical models of aggressive meningioma

Craig Horbinski, Guifa Xi, Yufen Wang, Rintaro Hashizume[✉], Mahesh Gopalakrishnan, Joanna J. Phillips, Peter Houghton, Charles D. James, and John A. Kalapurakal

Department of Neurological Surgery, Feinberg School of Medicine, Northwestern University, Chicago, Illinois, USA (C.H., G.X., C.D.J.); Department of Pathology, Feinberg School of Medicine, Northwestern University, Chicago, Illinois, USA (C.H.); Department of Radiation Oncology, Feinberg School of Medicine, Northwestern University, Chicago, Illinois, USA (Y.W., M.G., J.A.K.); Department of Pediatrics, Feinberg School of Medicine, Northwestern University, Chicago, Illinois, USA (R.H.); Departments of Neurological Surgery and Pathology, University of California San Francisco, San Francisco, California, USA (J.J.P.); Greehey Children's Cancer Research Institute, University of Texas at San Antonio, San Antonio, Texas, USA (P.H.)

Corresponding Author: Craig Horbinski, MD, PhD, Department of Neurological Surgery, Feinberg School of Medicine, Northwestern University, SQ6-518, 303 East Superior Street, Chicago, IL 60611, USA (craig.horbinski@northwestern.edu).

Abstract

Background. Meningiomas are the most common tumor arising within the cranium of adults. Despite surgical resection and radiotherapy, many meningiomas invade the brain, and many recur, often repeatedly. To date, no chemotherapy has proven effective against such tumors. Thus, there is an urgent need for chemotherapeutic options for treating meningiomas, especially those that enhance radiotherapy. Palbociclib is an inhibitor of cyclin-dependent kinases 4 and 6 that has been shown to enhance radiotherapy in preclinical models of other cancers, is well-tolerated in patients, and is used to treat malignancies elsewhere in the body. We, therefore, sought to determine its therapeutic potential in preclinical models of meningioma.

Methods. Patient-derived meningioma cells were tested *in vitro* and *in vivo* with combinations of palbociclib and radiation. Outputs included cell viability, apoptosis, clonogenicity, engrafted mouse survival, and analysis of engrafted tumor tissues after therapy.

Results. We found that palbociclib was highly potent against p16-deficient, Rb-intact CH157 and IOMM-Lee meningioma cells *in vitro*, but was ineffective against p16-intact, Rb-deficient SF8295 meningioma cells. Palbociclib also enhanced the *in vitro* efficacy of radiotherapy when used against p16-deficient meningioma, as indicated by cell viability and clonogenic assays. *In vivo*, the combination of palbociclib and radiation extended the survival of mice bearing orthotopic p16 deficient meningioma xenografts, relative to each as a monotherapy.

Conclusions. These data suggest that palbociclib could be repurposed to treat patients with p16-deficient, Rb-intact meningiomas, and that a clinical trial in combination with radiation therapy merits consideration.

Key Points

- Palbociclib enhances radiation activity against meningiomas.
- Palbociclib is most effective when meningioma cells are p16-deficient, Rb-intact.
- These data support a clinical trial in patients with high-risk meningiomas.

Importance of the Study

Despite the potential of chemotherapies to reach meningiomas, to date no such drugs have been shown to work against recurrent and high-grade meningiomas. These data suggest that the combination of palbociclib and radiotherapy is more effective in controlling the growth of aggressive meningiomas than either

modality in isolation. As in other contexts, palbociclib is most effective when meningioma cells are p16-deficient and Rb-intact. Since palbociclib is so well-tolerated by patients and is already used to treat other cancers, these data support a clinical trial in patients with high-risk meningiomas.

Meningiomas are the most common tumor arising within the cranial vault, at an overall age-adjusted incidence of approximately 19/100000 adults over the age of 40.¹ Meningioma incidence increases with advancing age, exceeding 40/100000 in people 75 years and older; incidence is also higher among women and blacks.¹ An estimated 35000 meningiomas will be diagnosed in 2020, about 81% of which are World Health Organization (WHO) grade 1, 17% are grade 2, and 2% are grade 3.¹

Meningiomas arise from meningeothelial cells of the arachnoid membrane surrounding the brain, and not the brain itself.² Consequently, meningiomas are not protected by the blood-brain barrier, in contrast to gliomas. And, unlike most gliomas, even invasive meningiomas do not diffusely infiltrate through the brain on a single-cell basis, but rather push into the brain as contiguous, cohesive extensions of the main tumor. Therefore, meningiomas should, in principle, be more accessible to systemically administered therapies. Yet the basic strategy for treating high-risk meningioma—surgery and radiotherapy (RT)—has not substantially changed over the past 50+ years. This works reasonably well for asymptomatic grade 1 meningiomas, which are generally followed with imaging surveillance, while symptomatic growing tumors are managed surgically.³ However, the management of grade 2–3 meningiomas is surgery followed by either observation, radiosurgery (12–16 Gy), or RT (54–60 Gy) for grade 2 tumors, and higher doses of RT (60 Gy) for grade 3 tumors.^{3–6} Despite this, patients with higher-risk tumors have high rates of tumor progression and eventual cancer-associated mortality.^{4–6} To date, there have been no chemotherapies or targeted agents that have proven efficacious against these high-risk tumors.^{7,8} Better strategies against high-risk meningiomas, especially ones that can act in concert with RT, are therefore needed.

Palbociclib is a well-tolerated, selective inhibitor of cyclin-dependent kinases 4 and 6 (CDK4/6). In phases G₀ and G₁ of the cell cycle, unphosphorylated Rb prevents E2F from triggering the transcription of genes required for progression into S phase of the cell cycle.⁹ When Rb is phosphorylated by CDK4/6, it dissociates from E2F, enabling S phase transition.¹⁰ The p16 protein, encoded by *CDKN2A/B*, prevents this by blocking CDK4/6. Many cancers either eliminate p16 or Rb, or amplify *CDK4*, in order to subvert the G1 arrest effect of Rb. Thus, tumors with reduced or absent p16 expression are generally more sensitive to palbociclib, whereas inactivation of Rb (e.g., by *RB1* deletion) renders tumor cells insensitive to palbociclib. In meningiomas, methylation or deletion of *CDKN2A/B*, and/

or a lack of nuclear p16 immunostaining, is more common with increasing grade and recurrence, whereas loss of Rb is very uncommon in meningiomas.^{11–16}

Palbociclib is the most extensively used CDK4/6 inhibitor in cancer clinical trials (according to <https://clinicaltrials.gov/>), it has already been FDA-approved for treating hormone-positive breast cancers and is currently being evaluated for the treatment of other malignancies.¹⁰ Preclinical research, in our group and others, showed that the administration of palbociclib during and after RT extended the survival of mice bearing intracranial tumor xenografts of gliomas and embryonal tumors, beyond that of RT alone.^{17–19} We therefore sought to determine whether palbociclib might have similar effects in high-risk meningiomas.

Materials and Methods

Tumor Cell Sources and Cultures

CH157 and IOMM-Lee cell lines were obtained from the American Type Culture Collection, and were propagated as monolayers in complete medium consisting of Dulbecco's modified Eagle medium (DMEM) supplemented with 10% fetal bovine serum (FBS) and non-essential amino acids. SF8295 cells were established from a University of California San Francisco surgical specimen through an approved Committee on Human Research protocol, and were maintained as a monolayer culture in DMEM with 10% FBS. All cells were cultured in an incubator at 37°C in a humidified atmosphere containing 95% O₂ and 5% CO₂. The unique identity of each cell line was annually authenticated by short tandem repeat analysis in CDJ's laboratory.

To enable cells for *in vivo* bioluminescence imaging (BLI), lentiviral vectors containing firefly luciferase were generated as previously described,²⁰ and were used to transduce CH157 and IOMM Lee cells. The cells were screened *in vitro* for transduction efficiency and luciferase activity by treatment with luciferin (D-luciferin potassium salt, 150 mg/kg, Gold Biotechnology) and analyzed for luminescence using a Synergy 2 Microplate Reader (BioTek Instruments Inc.).

Cell Proliferation

Tumor cells were cultured in the presence of 0, 0.001, 0.01, 0.1, 1, 10, or 100 μM palbociclib (Pfizer) for 72h. Viable cells

were assessed with MTS assay (Promega). All in vitro assays and analyses were performed at least triplicate, with mean and SD values plotted with GraphPad Prism 8.0 (GraphPad Prism) from the results of each type of analysis.

Real-Time PCR

Total RNA was isolated with the RNeasy Mini Kit (Cat#74106, Qiagen). cDNA was synthesized with qScript cDNA SuperMix (5 ×) (Cat#84034, Quanta Biosciences) following real-time (RT) PCR using Bio-Rad CFX96 Real-time PCR detection system with human specific NF2 primers from Qiagen (Cat#330001 PPH00203A) and from Integrated DNA Technologies NF2: forward 5'-cgggtccttgatcgtgtactg-3' and reverse 5'-tcaattgagatgaagtggaa-3' primers and GAPDH forward 5'-acagtccatccatcactgcc-3' and reverse 5'-gcctgcttcaccacctcttg-3' primers. To ensure accuracy, an internal reference reaction was performed on the same sample as used for the target gene. The results were standardized with the formula: $\Delta CT = CT_{Ref} - CT_{Target}$ and converted to folds of target gene over reference gene ($F = 2^{-\Delta CT}$). Data from a minimum of three independent experiments was used to quantify gene expression.

Immunoblotting

Cell lysates were collected from asynchronously proliferating cells using RIPA lysis buffer (Cell Signaling Technologies) supplemented with protease (Life Technologies Inc.) and phosphatase (Sigma) inhibitor cocktails. Lysates were resolved by sodium dodecyl sulfate polyacrylamide gel electrophoresis and transferred to nitrocellulose membranes. After probing with primary antibodies, the membranes were incubated with horseradish peroxidase-conjugated secondary antibody and visualized by ECL (Thermo Fisher) using Bio-Rad imaging work station (Bio-Rad Laboratories). Antibodies specific for NF2/Merlin (#6995), RB (4H1, #9309), phospho-RB (p-RB, Ser780, #9307) were obtained from Cell Signaling Technologies. Antibody for p16 was from BD Pharmingen (#554079), and β -actin antibody was from Sigma (#05-661).

Clonogenic Assay

Cells were seeded into 6-well tissue culture plates and allowed to adhere. Attached cells were irradiated (1, 2, 4 or 10 Gy) and treated with palbociclib at 10 nM 2 hours after irradiation. Radiation was delivered by a ^{137}Cs source (Mark I, model 68A irradiator, JL Shepherd & Associates). Cells were incubated with palbociclib for 1 week, at which time colonies were counted following staining with methylene blue (0.66% solution in 95% ethanol). Plating efficiencies were calculated as the ratio of the number of colonies formed to the number of cells seeded. Colonies of >50 cells were counted for surviving fraction determinations. Surviving fractions were calculated as the plating efficiency of treated cells divided by the plating efficiency of control cells. Dose enhancement factors were calculated at 10% survival.

Cell Cycle Distribution and Apoptosis Analyses

Mono- or combination treatment with palbociclib and radiation effects on the cell cycle distributions and apoptosis were determined by treating cells with 2Gy RT, followed by treatment with or without 1 μM palbociclib 3 hours later. Cells were harvested at 18 hours after RT, then counterstained with propidium iodide (PI) (Cat#P1304MP, Invitrogen) for cell cycle distributions. At 72 hours, cells were stained with PO-PRO-1 and 7-aminoactinomycin D (Cat#V35123, Invitrogen). Both cell cycle and apoptosis analyses were done using a BD FACSymphony flow cytometer. Non-treated cells served as controls. Cell cycle distributions were determined using Modfit LT for windows software (Verity Software House, version 5.0.9), and apoptosis data was analyzed using FlowJo software (Version 10.6.1, FlowJo LLC.).

In Vivo Studies

Six-week-old athymic nude mice (NCR-Foxn1^{nu}) were purchased from Envigo. All mice were housed under aseptic conditions, which included filtered air and sterilized food, water, bedding, and cages. The Northwestern Institutional Animal Care and Use Committee (IACUC) approved all animal protocols. CH157 or IOMM-Lee cells (2×10^5 cells) were implanted under the skull in the right frontal subdural region approximately 2 mm posterior to the bregma and 1 mm to the right of midline and to a depth of 3 mm from the bone surface. Engrafted mice were imaged 1–2 times weekly by bioluminescence imaging (BLI), as previously described.²¹ BLI was performed by subcutaneous injection with 150 mg/kg D-luciferin potassium (Gold Biotechnology) in mice anesthetized via 2.5% isoflurane; each mouse was imaged 10 min after luciferin injection on an IVIS SPECTRUM imaging station (Caliper Life Science) coupled to Living Image data-acquisition software. Intracranial signal intensities were quantified within regions of interest defined by the Living Image software. Bioluminescence measurements for each animal were normalized against their own corresponding bioluminescence obtained at the beginning of therapy. Animals were euthanized by CO₂ asphyxiation followed by cervical dislocation when they became moribund (e.g. >20% weight loss, neurologic symptoms, or evidence of pain/distress).

Radiation Therapy Quality Assurance (QA)

Meningioma xenografts were irradiated using a Gammacell[®] 40 Exactor ^{137}Cs source irradiator that has an average gamma ray energy of 660 keV and a central dose rate of 1Gy/min. We performed a number of RT QA initiatives to improve the precision and accuracy of RT dose delivery consistent with national standard.²² Dose rate calibrations were done per the American Association of Physicists in Medicine Task Group 61 (AAPM TG 61) protocol using an Accredited Dosimetry Calibration Lab (ADCL) calibrated ion chamber.²³ Calibrations were performed at the mid plane of the irradiation geometry for Cs irradiator using a 0.6cc volume ion chamber in air.²⁴

Dose uniformity studies using Gafchromic™ film were carried out and the dose variation across the beam was determined to be 7–10% per the machine specifications.

In addition to establishing an ADCL traceable dosimetry program, an experiment specific mouse phantom irradiation was also performed. Mouse phantoms with

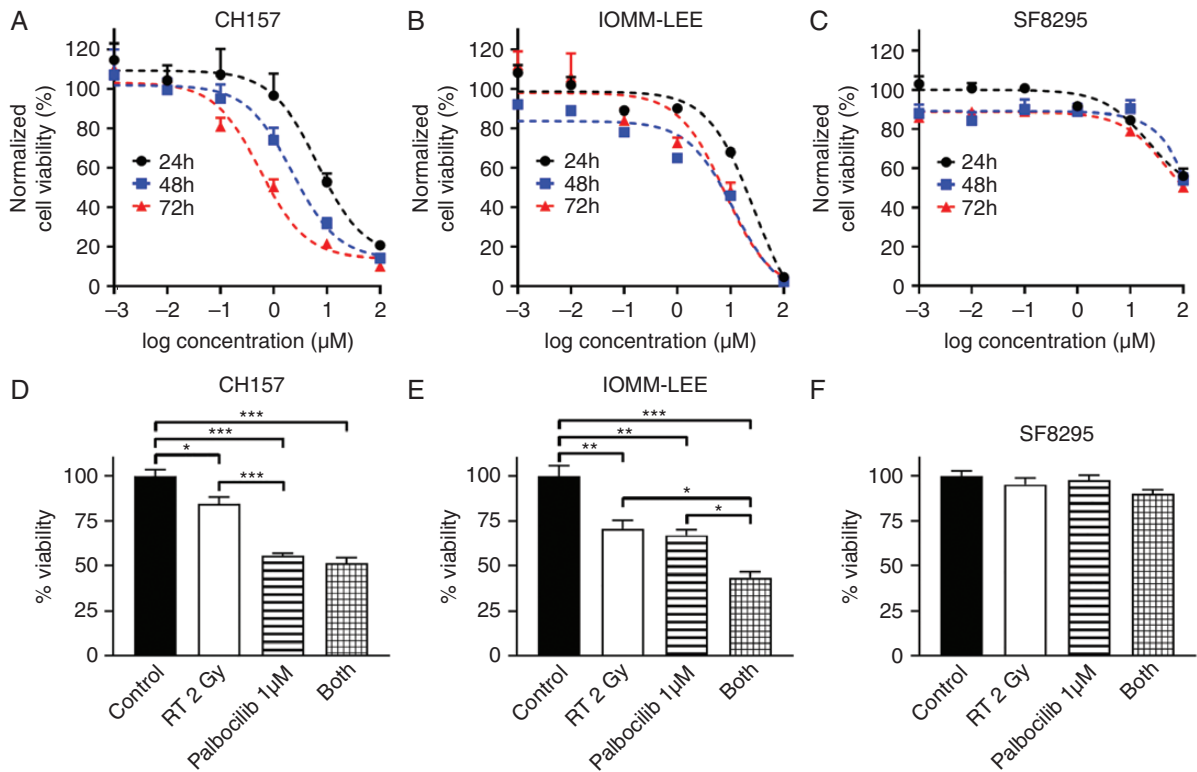


Figure 1. *In vitro* activity of palbociclib against meningiomas. (A–C) Dose-response curves showing viability of CH157 (A), IOMM-Lee (B), and SF8295 (C) meningioma cells treated with palbociclib. (D–E) Cell viability of CH157 (A), IOMM-Lee (B), and SF8295 (C) meningioma cells at 72 h time point after RT and/or palbociclib.

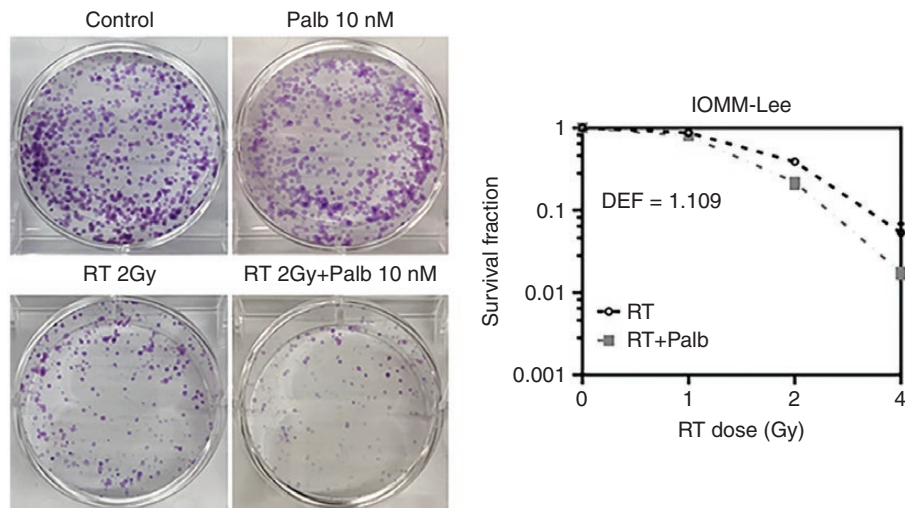


Figure 2. Effects of palbociclib and RT on clonogenicity of meningioma cells. Clonogenic assay results showing mono- and combination treatment effects on IOMM-Lee colony formation after seeding 1000 cells and at 1 week post administration of treatments. DEF: dose enhancement effect.

embedded Optically Simulated Light Detectors (OSLD) were procured from ADCL Lab which are calibrated and maintained by ADCL Lab. Irradiation of these mouse phantoms was done using a 2-field arrangement and the dose was prescribed to the midplane of the target volume. A field margin of 3–5 mm was applied around the target for a uniform and accurate dose delivery. To protect normal tissues outside the intended treatment area, Cerrobend blocks were fabricated with a thickness of 5 HVLs (Half value layer). The results from the OSLD doses in the treatment region were within 7% of the prescribed dose.

Statistical Analyses

Differences between mean values of two groups were compared using a two-sample *t*-test, or between multiple groups by one-way analysis of variance (ANOVA) and post hoc Tukey's test; *P* values less than 0.05 were considered significant. Kaplan-Meier and *t*-tests were performed to compare survival between groups. Graph generation and statistical analyses were performed with GraphPad PRISM 8 software.

Results

To evaluate the activity of palbociclib against meningiomas, we used three patient-derived models: CH157, IOMM-Lee, and SF8295. The first two are from WHO grade 3 anaplastic meningiomas. SF8295 was obtained from an 81-year-old male with recurrent meningioma that had progressed from grade 2 to 3, and which had undergone repeated surgeries for recurrences. IOMM-Lee is *NF2*-intact, whereas SF8295 and CH157 are *NF2*-deleted (Supplementary Figure S1A–B). Both CH157 and IOMM-Lee are p16-deficient and Rb-intact, whereas SF8295 expresses p16 but not Rb (Supplementary Figure S1A). Palbociclib suppressed Rb phosphorylation in CH157 and IOMM-Lee cells (Supplementary Figure S1C), and showed potent anti-proliferative effect against those cell lines *in vitro*, across 24–72h time points (IC_{50} against CH157 = 4.1–4.9 μ M, IC_{50} against IOMM-Lee = 9.2–15.2 μ M) (Figure 1A, B, Supplementary Figure S2A–B). In contrast, palbociclib showed little anti-proliferative effect against Rb-deficient SF8295 cells (IC_{50} = 154.9–1698 μ M) (Figure 1C, Supplementary Figure S2C). Whereas the combination of 1 μ M palbociclib and 2 Gy RT showed similar effect in reducing *in vitro* CH157 viability as palbociclib alone (Figure 1D), the combination had superior activity against IOMM-Lee cells relative to either treatment in isolation (Figure 1E). SF8295 cells, in contrast, were resistant to both treatments, alone as well as in combination (Figure 1F). IOMM-Lee cells, which adapted well to colony formation analysis (unlike CH157 cells), were tested by clonogenic assay for response to singular and combination treatments. In that setting, palbociclib enhanced the effect of low dose RT against colony formation (Figure 2). Together, these data suggest that palbociclib enhances the *in vitro* activity of RT against high-grade, Rb-intact meningiomas.

To assess the activity of palbociclib *in vivo*, luciferase-modified CH157 cells were used to establish intracranial tumors in athymic mice. RT, administered in 2 Gy fractions/day for 5 consecutive days, delayed tumor growth (Figure 3A, B) and significantly extended the survival of engrafted mice; palbociclib, administered at 150 mg/kg/day for 7 days, had a similar effect (Figure 3). The combination of RT + palbociclib delayed growth and extended median survival further than either modality used in isolation, although this reached statistical significance for

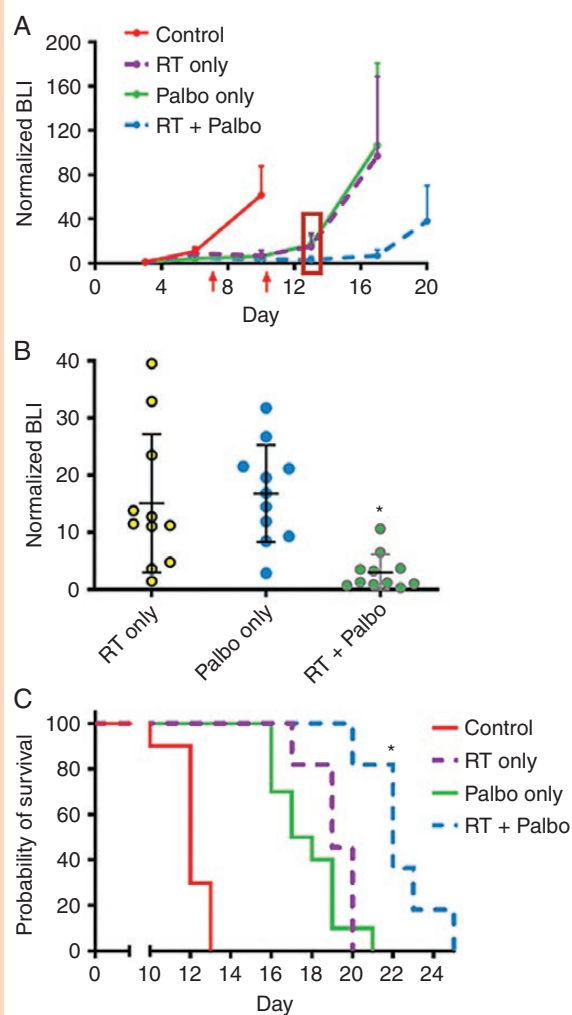


Figure 3. *In vivo* activity of palbociclib and hypofractionated RT against CH157 meningiomas. BLI monitoring (A & B) and survival analysis (C) of mice with intracranial CH157 tumor, and treated with RT only, palbociclib only, or RT + palbociclib. RT administered days 3–7 post tumor cell injection: 2 Gy/day × 5 days. Palbociclib administered days 3–10 post tumor cell injection 150 mg/kg/day. The first red arrow in (A) indicates the last day of RT. The second red arrow indicates the last day of Palbociclib. In (B), **P* < 0.01 for tumor bioluminescence of RT + palbociclib mice vs. RT only or palbociclib only mice in (B), as determined at 3 days following completion of palbociclib administration (indicated by the red rectangle in (A)). For (C), **P* < 0.05 for all two-way survival comparisons, except for RT only vs. RT+palbociclib (*P* = 0.17). *N* in (C) = 10 mice per group for control and palbociclib only, *N* = 11 for RT and RT + palbociclib.

survival only in comparison with palbociclib monotherapy (Figure 3C). While the effects of RT and palbociclib monotherapies were somewhat less pronounced in IOMM-Lee xenografts, the RT + palbociclib combination significantly delayed tumor growth (Figure 4A) and extended animal subject survival to a greater extent than either monotherapy (although as in CH157, this was statistically significant for survival only in comparison to palbociclib) (Figure 4B). Histologic analysis of treated CH157 and IOMM-Lee tumors showed that tumor growth delay from combination treatment was due to suppressed cell proliferation (Figure 5A, B); no significant difference in apoptotic response was observed between any of the treatment groups, either *in vivo* (Figure 5C) or *in vitro* (Supplementary Figure S3).

To determine the effect of palbociclib when used in combination with single high dose radiation using clinical radiosurgery equivalent doses, as opposed to the fractionated regimen used in the initial CH157 and IOMM-Lee experiments (Figures 3 and 4), mice intracranially engrafted with CH157 cells were treated with 10 Gy RT only, administered once, palbociclib only (100 mg/kg/day for 14 consecutive days), or the combination of single high dose RT + palbociclib. Combination treatment had the most substantial effect in extending animal subject survival (Figure 6A). Importantly, bioluminescence monitoring revealed a rapid increase in tumor bioluminescence on completion of the 2-week course of palbociclib administration in the combination treatment group (Figure 6B), suggesting that survival benefit from including palbociclib + RT could be extended by ongoing palbociclib administration.

Discussion

Despite the widespread assumption that meningiomas are a benign tumor, necessitating only surgical management

with or without RT, a large proportion of these tumors are lethal. In a phase II NRG clinical trial (RTOG 0539), among 52 patients with intermediate-risk meningioma (defined as newly diagnosed grade 2 after gross total resection or recurrent WHO grade 1) who were treated with RT (54 Gy), 3-year local control, progression-free survival (PFS), and overall survival (OS) rates were 96%, 94%, and 96%, respectively.³ However, among 53 patients with high-risk meningioma (defined as grade 3 and recurrent grade 2, or new grade 2 tumor after subtotal resection) and treated with higher doses of RT (60 Gy), 3-year local control, PFS, and OS rates were only 69%, 59%, and 79%, respectively.⁴ Thus, the high relapse and mortality rates after current treatments necessitates the adoption of new strategies in high-risk meningiomas.

Our data specifically demonstrates that palbociclib and RT are generally more effective *in vitro* and *in vivo* against malignant meningiomas than either modality used in isolation. Further, our results indicate that the delayed growth associated with combination treatment is due to an anti-proliferative effect, with little indication of enhanced cell death as being responsible for extending animal subject survival from treatment with radiation and palbociclib. Our data also show combination benefit when palbociclib is combined with higher dose single fraction RT (10Gy). This experiment was undertaken to explore the rationale for combining palbociclib and single-fraction radiosurgery or hypofractionated stereotactic RT in patients with recurrent meningioma post-RT. Post-RT recurrent meningiomas are increasingly being treated with radiosurgery or fractionated RT with photons or protons, with 2-year local control rates of about 80% and low rates of necrosis.^{25–27}

Palbociclib and RT have been successfully combined in other preclinical and clinical contexts,^{10,17–19} though the reasons why this combination is effective are not fully clear. Homologous recombination (HR), which is one of two mechanisms that a cell uses to repair double strand

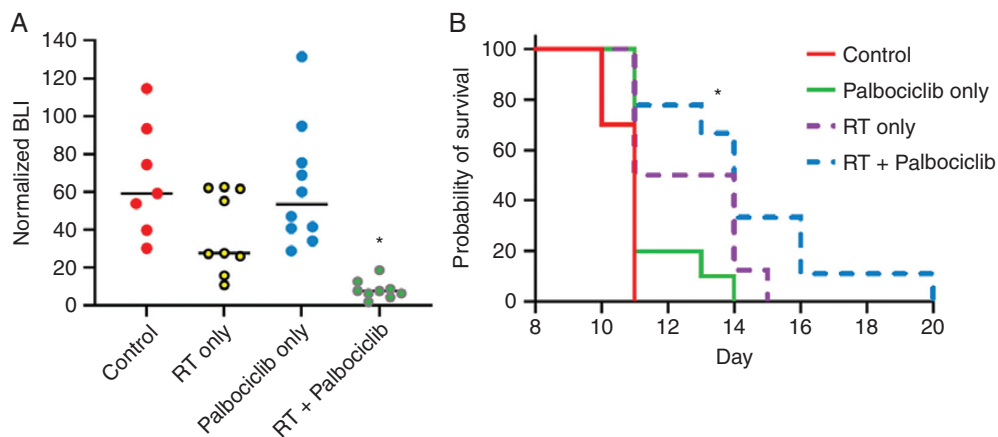


Figure 4. *In vivo* activity of palbociclib and hypofractionated RT against IOMM-Lee meningiomas. BLI (A) and survival (B) results for IOMM-Lee model. RT administered days 3–7 post tumor cell injection: 2 Gy/day × 5 days. Palbociclib administered days 3–10 post tumor cell injection 150 mg/kg/day. For (A), * $P < 0.001$ for RT + palbociclib vs. any other treatment group. For (B), * $P < 0.05$ for RT + palbociclib vs. control, and for RT + palbociclib vs. palbociclib only. $N = 7$ for control, 10 for palbociclib, 8 for RT, 9 for RT + palbociclib.

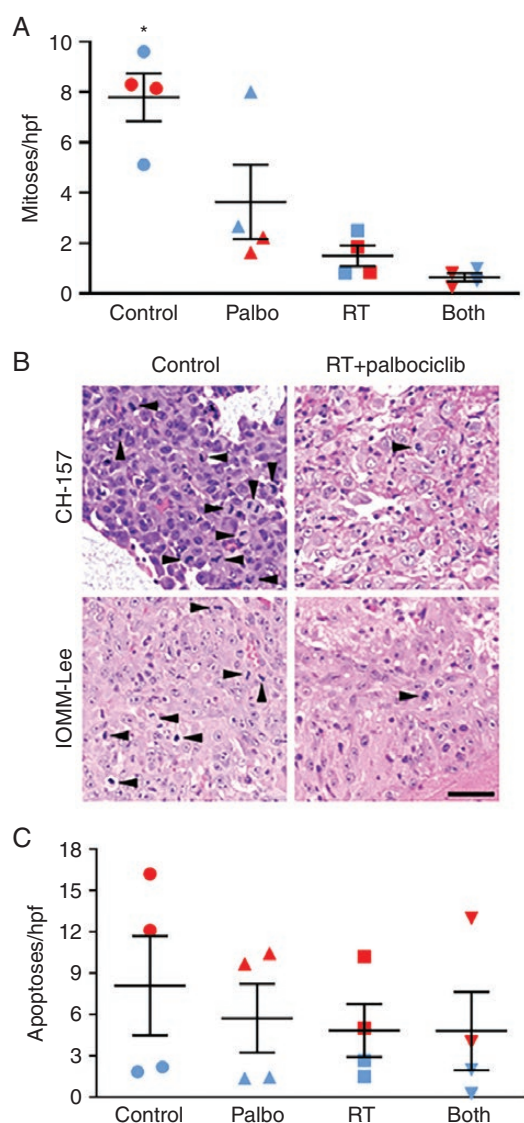


Figure 5. Tissue analysis of *in vivo* meningioma xenografts. (A) Mitosis counts in CH157 and IOMM-Lee intracranial tumors (open and filled symbols, respectively), following 5 days of radiation therapy (RT: 2 Gy/day \times 5), palbociclib therapy (150 mg/kg/day \times 5), or concurrent RT + palbociclib for 5 consecutive days. Each data point represents the average number of positive cells counted in 10 high-powered fields (400 \times) of a single intracranial tumor. * $P < 0.05$ versus all other groups, as indicated by one-way ANOVA analysis. (B) Representative photomicrographs of CH157 (upper panels) and IOMM-Lee (lower panels) intracranial xenografts. Mitoses are identified by arrowheads. Scale bar = 50 microns. (C) Same specimens as analyzed in (B), but examined for apoptotic cells, $P = 0.082$ via one-way ANOVA.

breaks, has activity during the late G2/S part of the cell cycle. Palbociclib, because of its ability to increase Rb function, blocks cell cycling at the G1/S phase checkpoint (Supplementary Figure S2). Thus, meningioma cells treated with palbociclib, which are stuck at the G1/S checkpoint, may be blocked from using HR to repair double strand breaks. This would be consistent with results

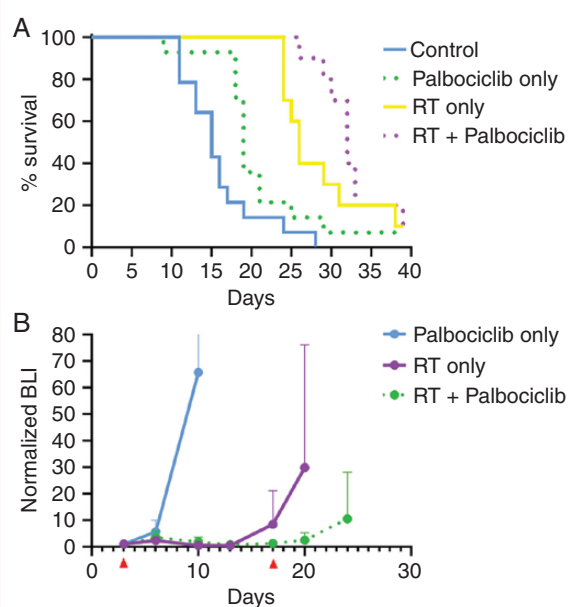


Figure 6. *In vivo* activity of palbociclib and single-dose RT against CH157 meningiomas. Survival (A) and BLI (B) results for mice engrafted with CH157, then assigned to one of the following groups: (i) control; (ii) 10 Gy RT only, administered once; (iii) palbociclib only (100 mg/kg/day for 14 consecutive days); (iv) combination of single high dose RT and 14 days of palbociclib. All intergroup comparisons in (A) produced $P < 0.05$ except for RT vs RT + palbociclib, which was $P = 0.167$. $N = 14$ for control and palbociclib, $N = 10$ for RT and RT + palbociclib.

from our previously published studies on ATRT, in which palbociclib extended the length of time that irradiated cells show unrepaired DNA double strand breaks.¹⁸ Another study, published by others, suggested that palbociclib inhibits protein phosphatase 5, in turn inhibiting the ability of ATM kinase to repair RT-induced DNA breaks.²⁸

Mice bearing either CH157 or IOMM-Lee xenografts survived longest when RT and palbociclib were administered together (Figure 3 and Figure 4). The response was even more striking in CH157 xenografts than IOMM-Lee, for reasons that remain unclear, although the *in vitro* IC_{50} was lower for CH157 cells than for IOMM-Lee cells (Figure 1A, B).

Recently, another group also reported that palbociclib + RT extended the survival of mice engrafted with either grade 3 or radiation-induced meningioma cells.²⁹ Compared to that study, unique features of the current work are as follows: (i) this study contains data from more meningioma models; (ii) palbociclib + RT was compared to RT alone; (iii) higher doses of RT were tested; (iv) other chemotherapies commonly used against gliomas were also tested against meningiomas and found to be ineffective (data not shown).

In sum, these data suggest that the combination of CDK4/6 inhibitors like palbociclib (with RT) is a potentially effective therapeutic strategy for high-risk meningiomas and support a biomarker-driven clinical trial for newly diagnosed high-risk meningioma patients, in which patients whose tumors are p16-deficient but pRb-intact would be treated with palbociclib and RT after surgical resection.

Supplementary Material

Supplementary material is available at *Neuro-Oncology Advances* online.

Keywords

meningioma | palbociclib | radiation

Funding

This work was supported by National Institute of Neurological Disorders and Stroke R01NS102669 and R01NS117104 (CH), the Northwestern University, National Cancer Institute P50CA221747 SPORE in Brain Tumor Research, the UCSF Brain Tumor SPORE Biorepository (NIH/NCI P50CA097257), and the Lou and Jean Malnati Brain Tumor Institute.

Acknowledgments

The authors thank Kathleen McCortney and Alicia Steffens of the Northwestern Nervous System Tumor Bank for histologic support. Thanks also to Aneta Baran of the Department of Neurological Surgery for animal model research support.

Conflict of interest statement. None of the authors have any conflicts of interest concerning the research in this manuscript.

Authorship Statement. Project conception: PH, CDJ, and JAK. Project implementation and data analysis: CH, GX, YW, RH, and JJP. Manuscript preparation: CH and GX. Manuscript edits: CH, CDJ, JAK, and MG.

References

- Ostrom QT, Patil N, Cioffi G, Waite K, Kruchko C, Barnholtz-Sloan JS. CBTRUS statistical report: primary brain and other central nervous system tumors diagnosed in the United States in 2013–2017. *Neuro Oncol.* 2020;22(12 Suppl 2):iv1–iv96.
- Louis DN, Perry A, Reifenberger G, et al. The 2016 World Health Organization classification of tumors of the central nervous system: a summary. *Acta Neuropathol.* 2016;131(6):803–820.
- Rogers L, Zhang P, Vogelbaum MA, et al. Intermediate-risk meningioma: initial outcomes from NRG Oncology RTOG 0539. *J Neurosurg.* 2018;129(1):35–47.
- Rogers CL, Won M, Vogelbaum MA, et al. High-risk meningioma: initial outcomes from NRG Oncology/RTOG 0539. *Int J Radiat Oncol Biol Phys.* 2020;106(4):790–799.
- Weber DC, Ares C, Villa S, et al. Adjuvant postoperative high-dose radiotherapy for atypical and malignant meningioma: a phase-II parallel non-randomized and observation study (EORTC 22042-26042). *Radiother Oncol.* 2018;128(2):260–265.
- Rydzewski NR, Lesniak MS, Chandler JP, et al. Gross total resection and adjuvant radiotherapy most significant predictors of improved survival in patients with atypical meningioma. *Cancer.* 2018;124(4):734–742.
- Preusser M, Brastianos PK, Mawrin C. Advances in meningioma genetics: novel therapeutic opportunities. *Nat Rev Neurol.* 2018;14(2):106–115.
- Buerki RA, Horbinski CM, Kruser T, Horowitz PM, James CD, Lukas RV. An overview of meningiomas. *Future Oncol.* 2018;14(21):2161–2177.
- Giacinti C, Giordano A. RB and cell cycle progression. *Oncogene.* 2006;25(38):5220–5227.
- Clark AS, Karasic TB, DeMichele A, et al. Palbociclib (PD0332991)-a selective and potent cyclin-dependent kinase inhibitor: a review of pharmacodynamics and clinical development. *JAMA Oncol.* 2016;2(2):253–260.
- Guyot A, Duchesne M, Robert S, et al. Analysis of CDKN2A gene alterations in recurrent and non-recurrent meningioma. *J Neurooncol.* 2019;145(3):449–459.
- Simon M, Park TW, Köster G, et al. Alterations of INK4a(p16-p14ARF)/INK4b(p15) expression and telomerase activation in meningioma progression. *J Neurooncol.* 2001;55(3):149–158.
- Boström J, Meyer-Puttitz B, Wolter M, et al. Alterations of the tumor suppressor genes CDKN2A (p16(INK4a)), p14(ARF), CDKN2B (p15(INK4b)), and CDKN2C (p18(INK4c)) in atypical and anaplastic meningiomas. *Am J Pathol.* 2001;159(2):661–669.
- Perry A, Banerjee R, Lohse CM, Kleinschmidt-DeMasters BK, Scheithauer BW. A role for chromosome 9p21 deletions in the malignant progression of meningiomas and the prognosis of anaplastic meningiomas. *Brain Pathol.* 2002;12(2):183–190.
- Korshunov A, Shishkina L, Golanov A. Immunohistochemical analysis of p16INK4a, p14ARF, p18INK4c, p21CIP1, p27KIP1 and p73 expression in 271 meningiomas correlation with tumor grade and clinical outcome. *Int J Cancer.* 2003;104(6):728–734.
- Tse JY, Ng HK, Lo KW, et al. Analysis of cell cycle regulators: p16INK4A, pRb, and CDK4 in low- and high-grade meningiomas. *Hum Pathol.* 1998;29(11):1200–1207.
- Hashizume R, Tom M, Ihara Y, et al. Preclinical investigation of concurrent vs. sequential radiation + cdk4/6 inhibitor therapy reveals heightened anti-tumor effect from inhibitor administration following completion of radiation. *Neuro Oncol.* 2013;15(s3):ET-037.
- Hashizume R, Zhang A, Mueller S, et al. Inhibition of DNA damage repair by the CDK4/6 inhibitor palbociclib delays irradiated intracranial atypical teratoid rhabdoid tumor and glioblastoma xenograft regrowth. *Neuro Oncol.* 2016;18(11):1519–1528.
- Barton KL, Misuraca K, Cordero F, et al. PD-0332991, a CDK4/6 inhibitor, significantly prolongs survival in a genetically engineered mouse model of brainstem glioma. *PLoS One.* 2013;8(10):e77639.
- Sarkaria JN, Yang L, Grogan PT, et al. Identification of molecular characteristics correlated with glioblastoma sensitivity to EGFR kinase inhibition through use of an intracranial xenograft test panel. *Mol Cancer Ther.* 2007;6(3):1167–1174.
- Ozawa T, James CD. Establishing intracranial brain tumor xenografts with subsequent analysis of tumor growth and response to therapy using bioluminescence imaging. *J Vis Exp.* 2010;13(41):1986.
- Desrosiers M, DeWerd L, Deye J, et al. The importance of dosimetry standardization in radiobiology. *J Res Natl Inst Stand Technol.* 2013;118:403–418.
- Ma CM, Coffey CW, DeWerd LA, et al.; American Association of Physicists in Medicine. AAPM protocol for 40-300 kV x-ray

- beam dosimetry in radiotherapy and radiobiology. *Med Phys*. 2001;28(6):868–893.
24. Hranitzky EB, Almond PR, Suit HD, Moore EB. A cesium-137 irradiator for small laboratory animals. *Radiology*. 1973;107(3):641–644.
 25. Lin AJ, Hui C, Dahiya S, et al. Radiologic response and disease control of recurrent intracranial meningiomas treated with reirradiation. *Int J Radiat Oncol Biol Phys*. 2018;102(1):194–203.
 26. Imber BS, Neal B, Casey DL, et al. Clinical outcomes of recurrent intracranial meningiomas treated with proton beam reirradiation. *Int J Part Ther*. 2019;5(4):11–22.
 27. Kim M, Lee DH, Kim Rn HJ, Cho YH, Kim JH, Kwon DH. Analysis of the results of recurrent intracranial meningiomas treated with re-radiosurgery. *Clin Neurol Neurosurg*. 2017;153:93–101.
 28. Huang CY, Hsieh FS, Wang CY, et al. Palbociclib enhances radiosensitivity of hepatocellular carcinoma and cholangiocarcinoma via inhibiting ataxia telangiectasia-mutated kinase-mediated DNA damage response. *Eur J Cancer*. 2018;102:10–22.
 29. Das A, Alshareef M, Martinez Santos JL, et al. Evaluating anti-tumor activity of palbociclib plus radiation in anaplastic and radiation-induced meningiomas: pre-clinical investigations. *Clin Transl Oncol*. 2020;22(11):2017–2025.